STUDIES OF EXCITABLE MEMBRANES

II. A Comparison of Specializations at Neuromuscular Junctions and Nonjunctional Sarcolemmas of Mammalian Fast and Slow Twitch Muscle Fibers

MARK H. ELLISMAN, JOHN E. RASH, L. ANDREW STAEHELIN, and KEITH R. PORTER

From the Department of Molecular, Cellular, and Developmental Biology, University of Colorado, Boulder, Colorado 80302, and the Department of Pharmacology and Experimental Therapeutics, University of Maryland School of Medicine, Baltimore, Maryland 21201

ABSTRACT

Mammalian fast and slow twitch skeletal muscles are compared by freeze-fracture, thick and thin sectioning, and histochemical techniques using conventional and high voltage electron microscopy. Despite gross morphological differences in endplate structure visualized at relatively low magnifications in thin sections, rat extensor digitorum longus (EDL) (fast twitch) and soleus (slow twitch) fibers cannot be distinguished on the basis of size, number, or distribution of molecular specializations of the pre- and postsynaptic junctional membranes exposed by freeze fracturing. Specializations in the cortex of the juxtaneuronal portions of the junctional folds are revealed by high voltage electron stereomicroscopy as a branching, ladder-like filamentous network associated with the putative acetylcholine receptor complexes. These filaments are considered to be involved in restricting the mobility of receptor proteins to the perineuronal aspects of the postsynaptic membrane. Although the junctional membranes of both EDL and soleus appear similar, a differential specialization of the secondary synaptic cleft was noted. The extracellular matrix in the bottom of soleus clefts was observed as an ordered system of filamentous "combs." These filamentous arrays have not been detected in EDL junctions.

Examination of the extrajunctional sarcolemmas of EDL and soleus reveal additional differences which may be correlated with variations in electrical and contractile properties. For example, particle aggregates termed "square arrays" previously described in the sarcolemmas of some fibers of the rat diaphragm were observed in large numbers in sarcolemmas of EDL fibers but were seldom encountered in soleus fibers. These gross compositional differences in the membranes are discussed in the light of functional differences between fiber types.

Mammalian skeletal muscles are composed of numerous individual fibers which are heterogene- ous with respect to a number of measurable parameters. Fiber "types" have been classified

according to variations in contractile properties (9, 12), histochemical staining patterns (8, 17, 27, 38), biochemical composition (3, 4, 53), electrophysiological properties (2, 37), and cytostructural detail (20, 24, 56). Whether these differing parameters are obligatorily or systematically interrelated has been the subject of continuing controversy since Ranvier (43) initially equated slow twitch contractions with red muscles and fast twitch contractions with white muscle.

Our recent freeze-fracture studies of muscle fiber membranes (22, 45, 47) demonstrate several new cytostructural parameters which may be of value in characterizing mammalian skeletal muscles and their innervating nerves on the basis of the macromolecular organization of the synaptic and nonsynaptic membrane systems. Freeze-fracture images of the presynaptic membranes of all endplates examined in the rat diaphragm exhibited paired rows of 100-A particles presumably involved in the release of transmitter. The postsynaptic membrane folds revealed characteristic irregular rows of particles aggregated at the tops of the folds close to the nerve terminal. Circumstantial evidence was assembled implicating the 110-140-A particles comprising these "herringbone rows" as the functional units for acetylcholine receptor activity. In addition, we described aggregates of 60-A particles in orthogonal arrays ("square arrays") in the nonjunctional sarcolemmas of many fibers from the diaphragm. In the present study, we have attempted to determine whether individual fibers from fast and slow contracting muscles can be distinguished on the basis of the macromolecular architecture of their presynaptic membranes, their postsynaptic junctional folds, or their nonjunctional sarcolemmas. To this end we have examined rat extensor digitorum longus (EDL) and rat soleus muscles. Rat EDL is comprised of a pure population of fast contracting twitch fibers; rat soleus, on the other hand, contains no fast fibers, but a mixture composed of approximately 80% slow and 20% intermediate fibers (11). Each of these muscles is therefore distinct in contractile properties, while containing intermixed populations of fibers according to other methods of classification (25).

Parametric aspects of the macromolecular specializations of these membranes are evaluated and correlated with quantitative information obtained by other techniques. The present data establish the occurrence of a variable membrane property (square arrays) whose occurrence may be related to stimulus characteristics, activity regimens, and/or trophic factors and thus may represent a new parameter for probing the complex nature of interactions between excitable cells.

MATERIALS AND METHODS

Five normal adult male albino rats (200–400 g) were fixed by whole-body perfusion according to methods previously described (45). Whole soleus and EDL muscles were removed from the left and right legs, dissected into small bundles containing 10–50 fibers, and stained for cholinesterase activity (45) in order to visualize the neuromuscular junction (NMJ). Carefully trimmed samples containing either a few neuromuscular junctions or portions of fibers at selected distances from the neuromuscular junctions (as shown in Fig. 1, below) were slowly equilibrated to 30% glycerol, placed on brass-mesh specimen supports, quickly frozen in liquid Freon 12, maintained at $-150°C$, and fractured and replicated at $-103°C$ on a Balzer's Freeze Etch device (Balzers, Principality of Liechtenstein). Replicas were prepared with either a conventional platinum-carbon gun, or the electron beam gun equipped with a time and heat-limiting shutter of our own design. The thickness of platinum coats was regulated by an interlocked quartz crystal thin film monitor.

After brief staining for cholinesterase activity, samples that were to be examined by conventional thin-section electron microscopy or HVEM stereoscopy were post-fixed in 1% OsO_4, stained en bloc with aqueous or methanolic uranyl acetate (57), dehydrated in methanol series, embedded in Epon, Araldite, DDSA (48), and poststained with lead citrate (59). Activated junctions were obtained by supramaximal stimulation (2/s–0.2 ms duration) delivered to an oil bath-isolated sciatic nerve. This was achieved by monitoring isometric twitch contraction times with a Grass FT03-6 force transducer (Grass Corp., Quincy, Mass.) tied to the distal tendon of either muscle. Nerve stimulation began at least 1 min before the perfusion process began. Muscular contractions were of consistent force until glutaraldehde was introduced; at this point the stimulus immediately ceased eliciting contraction. Conventional thin sections and replicas were examined at accelerating voltages of 80 or 100 kV in either a JEM-100B or Siemens Elmiskop 101 electron miscroscope. Stereoscopy of thin and thick sections was performed with the aid of the JEM-1000 high voltage electron microscope, at the National High Voltage Electron Microscope Facility, Boulder, Colo. We have incorporated the freeze-etch nomenclature recently adopted by Branton et al. (7), in which the protoplasmic fracture face is referred to as PF (formerly A face), and the extracellular fracture face is referred to as EF (formerly B face). Unless otherwise indicated, all calibration bars on figures represent 1 μm.
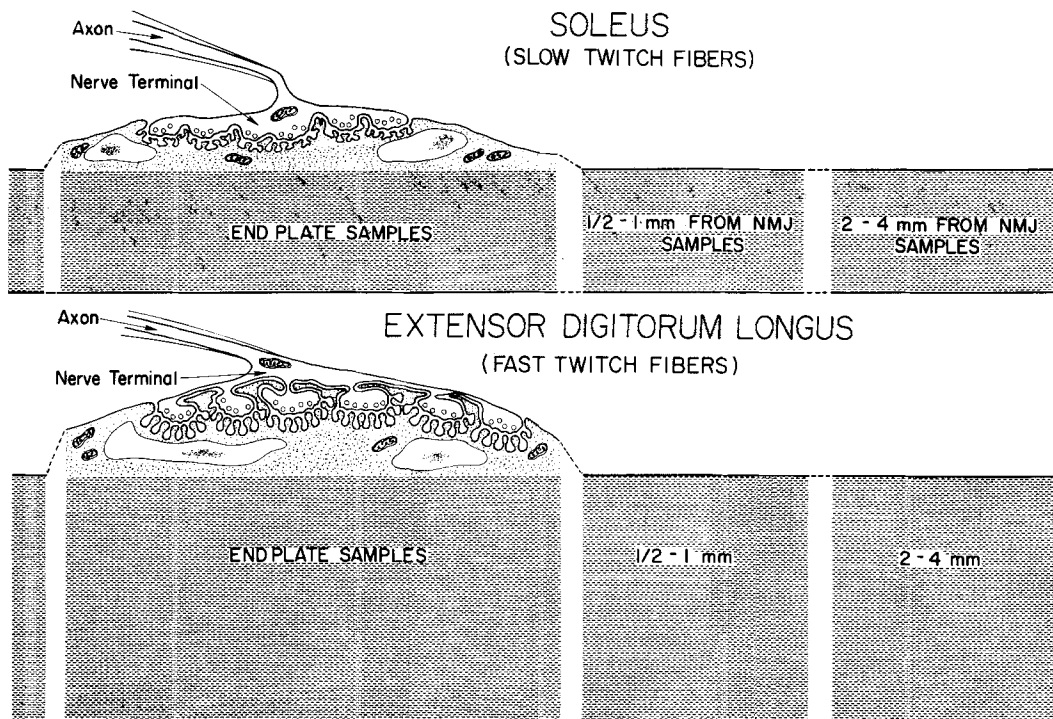
FIGURE 1 Semidiagrammatic representation of junctional differences between soleus and EDL fibers. The broad nerve terminal of soleus is apposed by relatively shallow irregular junctional folds. In contrast, the bulblike nerve terminal expansions of EDL fibers are apposed by more regular, deeper junctional folds. Also illustrated in this diagram are the various distances at which samples were taken for quantitative analysis of sarcolemmal specializations.

OBSERVATIONS

Comparisons of the Neuromuscular Junctions of Fast and Slow Twitch Fibers in Thin Sections

In thin sections parallel to the long axis of muscle fibers, the nerve terminals of soleus endplates usually resemble flattened plaques with vesicle-rich expansions interconnected by broad areas of filamentous neuroplasm (Fig. 2 a). The flattened ovoid endplates of soleus fibers are 30–50 μm in length and 20–30 μm in width. In contrast, the neuromuscular junctions of the larger EDL fibers consist of numerous lateral and terminal expansions arising from ramifications of the terminal branch of the motor axon (Fig. 3 a). The many anastomosing elements and bulblike terminal expansions result in larger ovoid endplates 75–100 μm in length, or one and a half to two times the dimensions of the endplates of soleus. In soleus fibers, the junctional folds (Fig. 2 b) are somewhat

broader and more irregular than those of EDL fibers (Fig. 3 b). The invaginations between folds are correspondingly of different dimensions—0.75 μm deep in soleus vs. 1 μm deep in EDL (see semidiagrammatic comparison, Fig. 1).

Presynaptic Membranes in Thin Sections

At intermediate magnification, neuromuscular junctions of both fibers (Figs. 2 b and 3 b) appear as a complex apposition of nerve and muscle membranes separated by the 400–600-Å synaptic cleft. Within the nerve terminals are numerous 500-Å synaptic vesicles, often arranged in small clusters adjacent to the presynaptic membrane immediately opposite the clefts between junctional folds (the "secondary cleft"). Cytoplasmic densities are observed associated with the presynaptic membrane of EDL and soleus fibers stained en bloc with methanolic uranyl acetate (Fig. 4 a, c, d). As shown in Fig. 4 a, these presynaptic densities are not always present at every opening of a secondary cleft. Vesicles often are observed em-
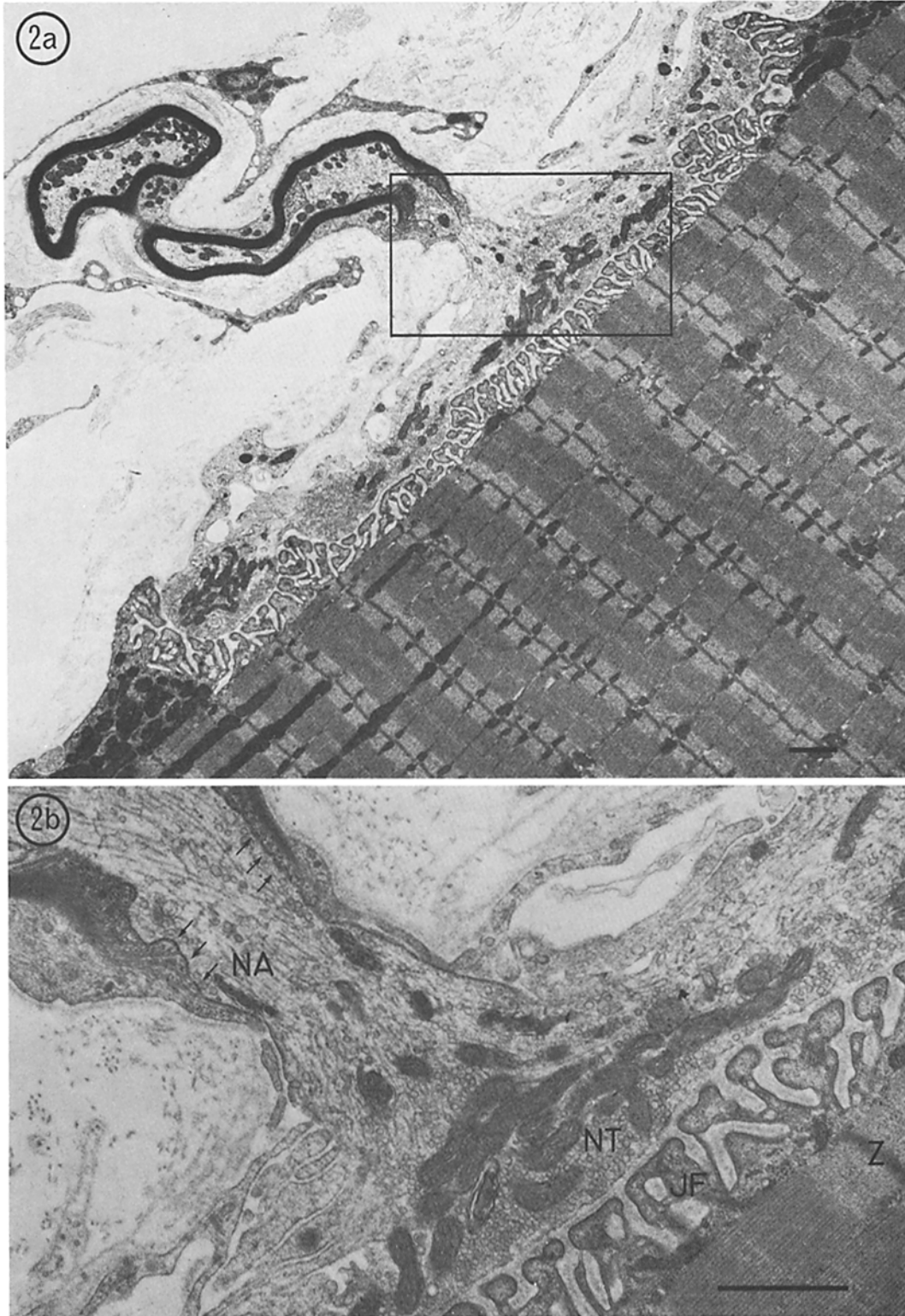
FIGURE 2 (a) Terminal branch motor axon innervating soleus muscle fiber. Note contiguity of vesicle-laden neuroplasm. × 7,500. (b) Serial section of area inscribed in Fig. 2 a. The terminal myelin loops (arrows) extend to within 5 μm of the shallow and irregular junctional folds (JF). Numerous neurofilaments and microtubules appear continuous from the large (1 μm) axon (NA) into the flattened nerve terminal (NT). (Compare the widths of the Z bands in soleus fibers and in EDL fibers in Fig. 2 b). × 20,000.
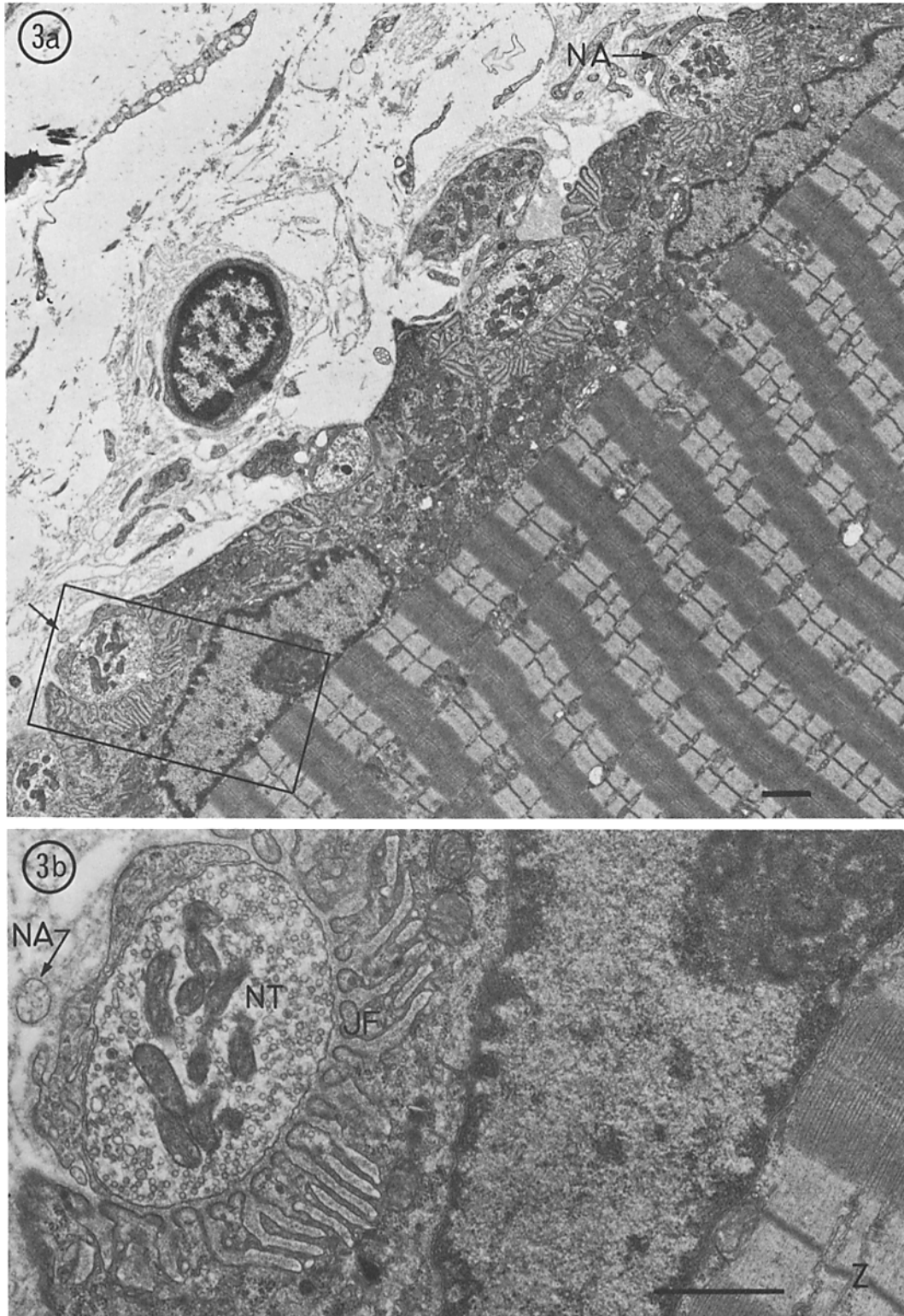
FIGURE 3 (a)   Bulblike terminal expansions comprising a portion of a neuromuscular junction of an EDL fiber. Note the characteristic subjunctional nuclei. × 7,500. (b) Higher magnification of area inscribed in Fig. 3 a. A single nerve terminal expansion (NT) is associated with numerous regular junctional folds (JF) of slightly greater depth than those seen in soleus. × 20,000

bedded in this presynaptic dense material, and as seen in Fig. 4 c are immediately adjacent to the neurolemma. Occasionally, thin sections reveal periodic projections from the neurolemma into the cytoplasm apparently associated with synaptic vesicles (arrows, Fig. 4 d). The relationship between similar presynaptic densities and vesicle attachment sites in amphibian neuromuscular junctions has been detailed by Couteaux and Pécot-Dechavassine (13), and therein the concept of "active zones" developed. Freeze-cleaving of the amphibian active zones recently reported by several investigators (16, 28, 42) has added the membrane molecular dimension to our understanding of the functional morphology involved in transmitter release. In mammalia, however, the membrane molecular organization of active zones is different from that of amphibia.
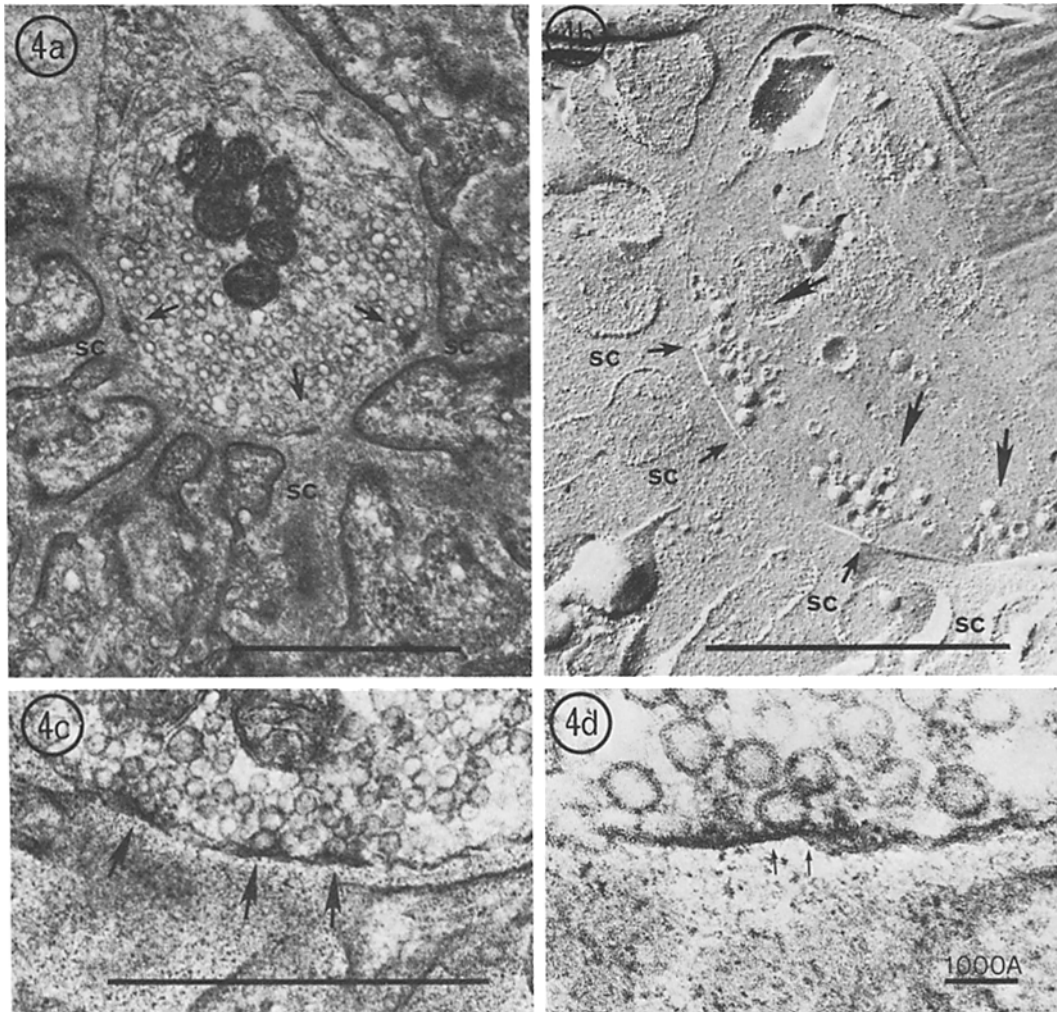

FIGURE 4 (a) Portion of soleus neuromuscular junction stained with methanolic uranyl acetate en bloc. Electron-dense areas (arrows) of presynaptic membrane are located opposite the secondary junctional cleft (SC). × 30,000. (b) Cross fracture of an activated EDL nerve terminal revealing synaptic vesicle aggregation (arrows) opposite the secondary clefts. Small arrows denote individual vesicles in close proximity to the presynaptic membrane. × 40,000. (c, d) Presynaptic membrane densities apparently associated with vesicle attachment. The densities appear to contain filamentous projections interconnecting the vesicles with the presynaptic membrane. Fig. 4 c, × 50,000; Fig. 4 d, × 125,000.

Presynaptic Membranes in Freeze-Fracture

In cross fracture (Fig. 4 b) the relationship between nerve terminal, synaptic vesicles, and junctional folds can be compared to equivalent images in thin section (i.e., Fig. 4 a). The periodicity of the postsynaptic junctional folding is sometimes represented by gentle undulations of the presynaptic membrane. A relatively large area of presynaptic membrane exhibiting this effect is depicted in Fig. 5. This imprinting is fortunate, for it allows one to note the consistent location of particulate specializations of the presynaptic membrane, relative to the postsynaptic junctional folding. Located on the tops of presynaptic ridges representing regions of membrane overlying the
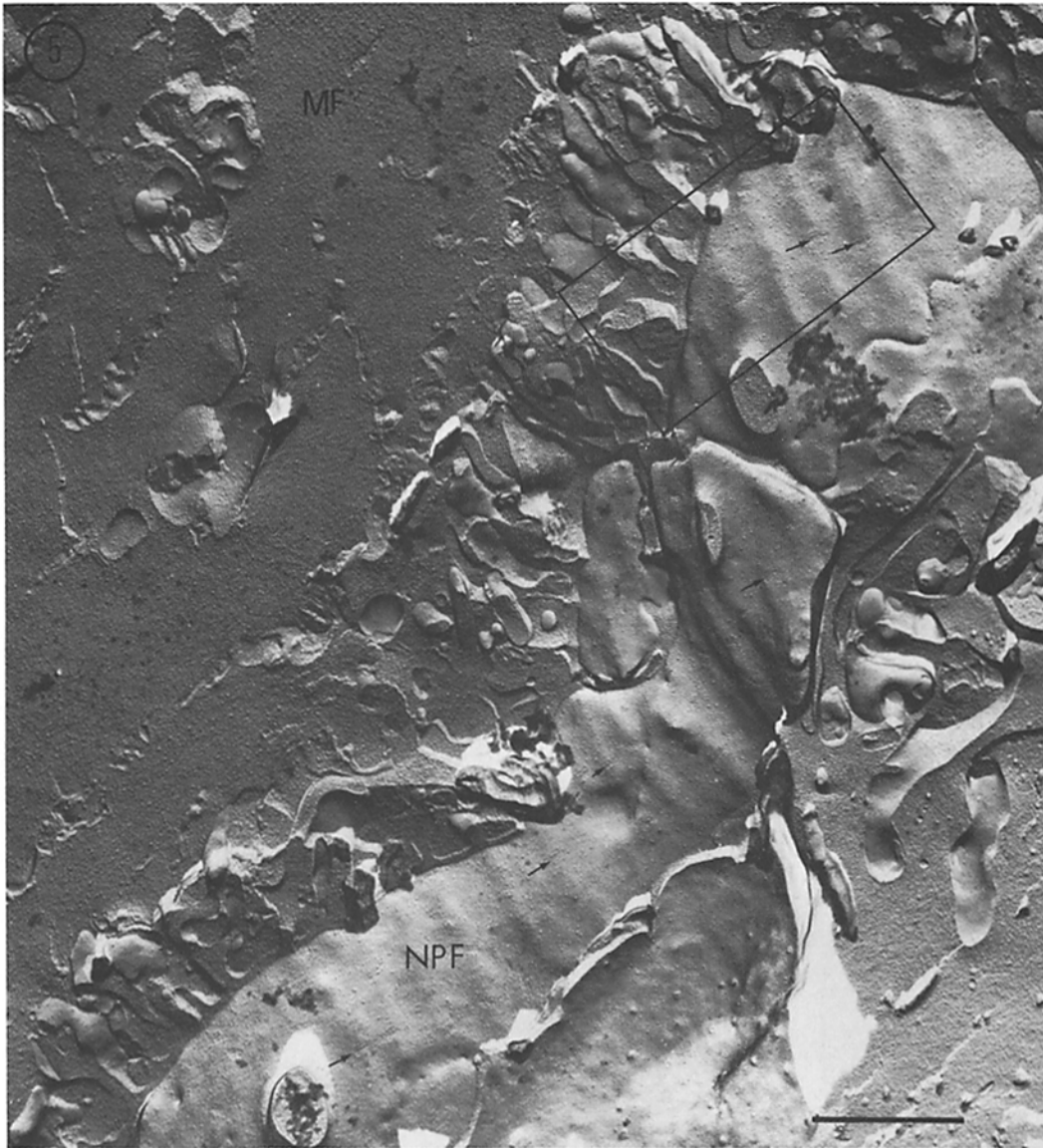

FIGURE 5 Cross fracture of EDL myofiber in the region of the motor endplate. In the protoplasmic fracture face of the two terminal nerve expansions (NPF), gentle ridges, associated with the secondary synaptic clefts, are observed to possess doublet arrays of 100-A particles (arrows). (MF = myofibrils in cross fracture). × 20,000.
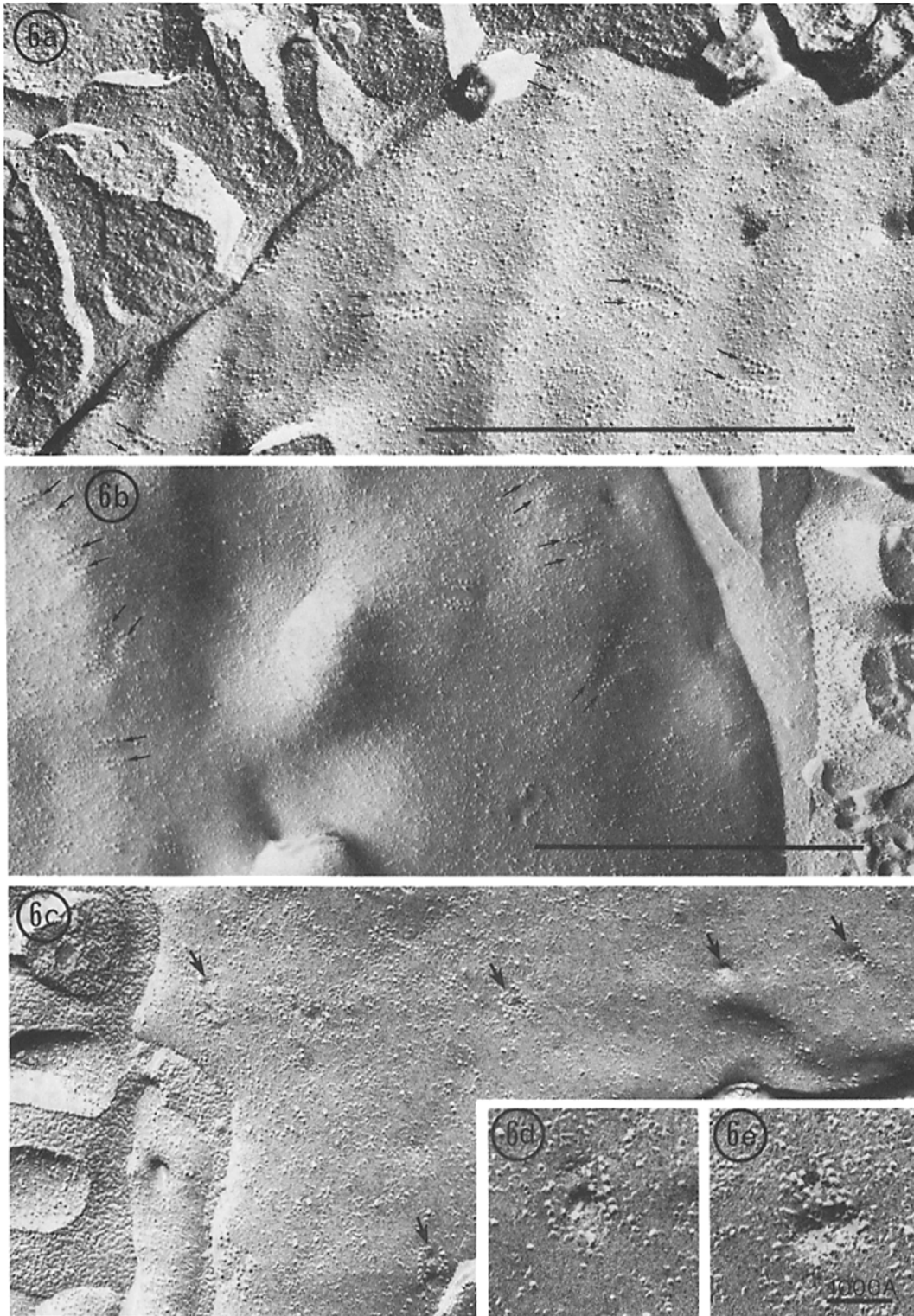
FIGURE 6 (*a*)   Higher magnification of inscribed area in Fig. 5. Paired doublet arrays primarily localized on crests associated with secondary clefts. × 65,000. (*b*) Quiescent endplate of soleus fiber, exhibiting bands of similar paired doublet arrays. × 50,000. (*c*) Active endplate demonstrating partial disruption of doublet arrays by presumed transmitter release process (arrows). × 50,000. (*d, e*) Higher magnification of selected doublet arrays demonstrating membrane disruption associated with stimulation. × 100,000.

759

secondary synaptic clefts are organized specializations of the membrane composed of paired double rows of 100-Å particles. Protoplasmic fracture faces (PF) of mammalian nerve terminal, therefore, are easily recognized by their complement of characteristic parallel double rows consisting of 6 to 10 100-A particles (Figs. 5, 6 a–c). In a nerve terminal not releasing transmitter these two parallel rows have an apparent 200-Å square lattice structure and are usually separated by approximately 400 A from an ajoining set of similar rows (Fig. 7 a). Although similar to the four presynaptic particle rows described for amphibia (16, 28, 42), the four rows in mammalia take up a different orientation with respect to the secondary cleft and are shorter. The long rows in amphibia run with and overlie the longest axis of the secondary cleft parallel to and between two adjacent postsynaptic folds. The much shorter rows in mammalia run with and overlie the shortest axis of the secondary cleft spanning the gap between two adjacent postsynaptic folds. Mammalian rows are therefore rotated 90° with respect to the postsynaptic membrane from the similar specialization in amphibia (Fig. 12). These specializations are similar in the presynaptic membranes of both EDL and soleus junctions (Fig. 6 a, b), and have approximately the same dimensions as the presynaptic densities observed in thin sections (Fig. 4 c, d).

A nerve terminal stimulated during fixation and therefore actively involved in the process of releasing transmitter during fixation reveals these rows of particles with a somewhat altered morphology (Fig. 6 c). In stimulated junctions a perturbance of the membrane is associated with these particles in the 400-Å space between the double rows (Figs. 6 c, 7 b). Depressions of 150–500-Å are observed, usually between the doublets, often disrupting the regularity and spacing of the particle rows (Fig. 6 d, e).
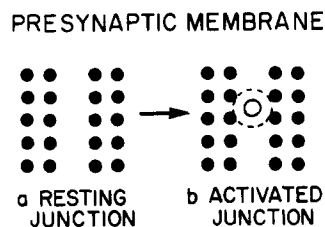
PRESYNAPTIC MEMBRANE

a RESTING   b ACTIVATED
JUNCTION   JUNCTION

FIGURE 7 a, b   Specializations of nerve terminal membrane a, in resting junction, and b, in junction activated during fixation.

Specialization of the Secondary Synaptic Clefts

The synaptic cleft can be easily identified by the dark histochemical reaction product of cholinesterase activity (Fig. 8 a). If the reaction product is allowed to wash out in the standard buffer solution (pH 7.2), a network of filaments lining the sides and lower portions of the clefts in soleus fibers (Fig. 8 b) becomes visible. Sections which transect the long axis of a secondary cleft (Fig. 8 c) reveal a row of cross-sectioned filaments lying parallel and external to the junctional fold membrane. Occasionally, a second layer of filaments is observed external to and at right angles to the first layer (Fig. 8 c, arrow). When both filamentous layers are included in a section tangential to the fold membrane (Fig. 8 d), a noninterwoven screen composed of two rows of filaments oriented at approximate right angles can be observed. This network of filaments has yet to be observed in EDL fibers.

Comparisons of the Postsynaptic Membranes by Freeze-Fracture

Often, the cleavage plane follows the contours of the postsynaptic membrane. This juxtaneural portion of the junctional fold membrane has been demonstrated to be the site of acetylcholine receptor activity (1, 23), and we have hypothesized (45) that the receptors are arranged in functional complexes at the tops of the folds, appearing as irregular rows of 110–140-Å particles (Figs. 9 a, b, 10, 14). These "herringbone rows" of particles on the protoplasmic fracture face terminate abruptly at about 25% of the depth of the folds, leaving particles of more varied diameters (80–140-Å) over the remaining lower 75% of the folds.

Despite gross structural variations between junctions of EDL and soleus fibers, no apparent differences were observed in the number and distribution of the characteristic macromolecular specializations observed at the tops of junctional folds (compare Fig. 9 a and 9 b of soleus with Figs. 10 and 14 a of EDL). These irregularly arrayed, putative ACh receptor complexes have identical packing densities of $1,800$–$2,300/\mu m^2$, with an average of $1,900$–$2,000/\mu m^2$.

The Junctional Fold in Sectioned Material

The thin section in Fig. 8 a illustrates the increased density of the postsynaptic membrane
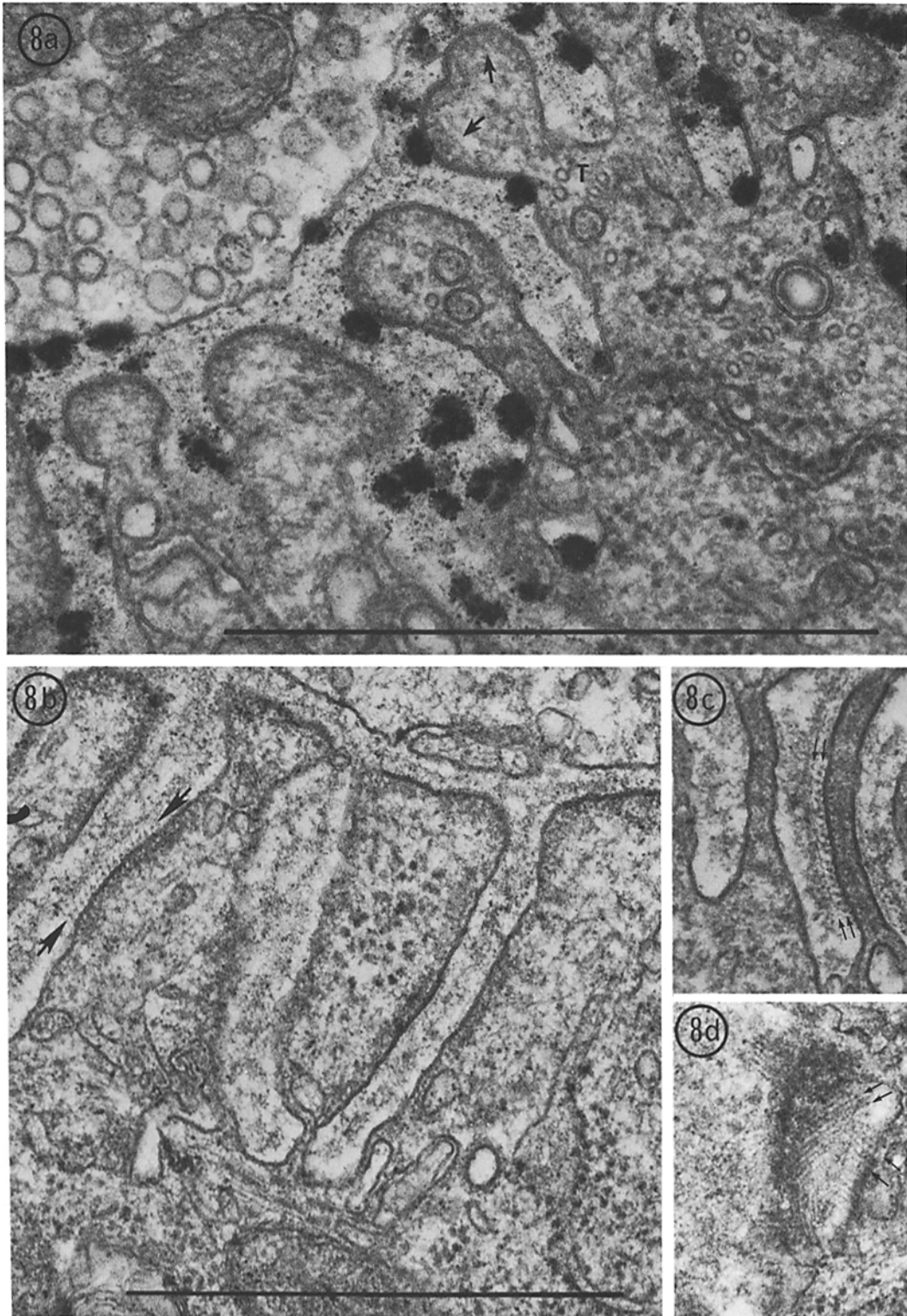
FIGURE 8 (a) Neuromuscular junction with electron-dense cholinesterase reaction products in synaptic cleft. The perineuronal, subplasmalemmal cytoplasm of the junctional fold contains filamentous and amorphous material of increased electron density (arrows). Note the numerous microtubules (T) in the junctional folds. Aqueous uranyl acetate *en bloc*. × 100,000. (b) Soleus endplates with electron-dense cholinesterase deposits removed by prolonged exposure to buffer solution. The extracellular filamentous matrix (arrows) was observed in all soleus fibers but has not been observed in EDL. × 75,000. (c) Ultrathin cross section of cleft and "combs" demonstrating cross and longitudinal orientation of the two nonoverlapping layers (arrows). Filaments oriented at approximate right angles. × 75,000. (d) Oblique section through secondary synaptic cleft and soleus "combs" demonstrating apparent meshwork. × 100,000.
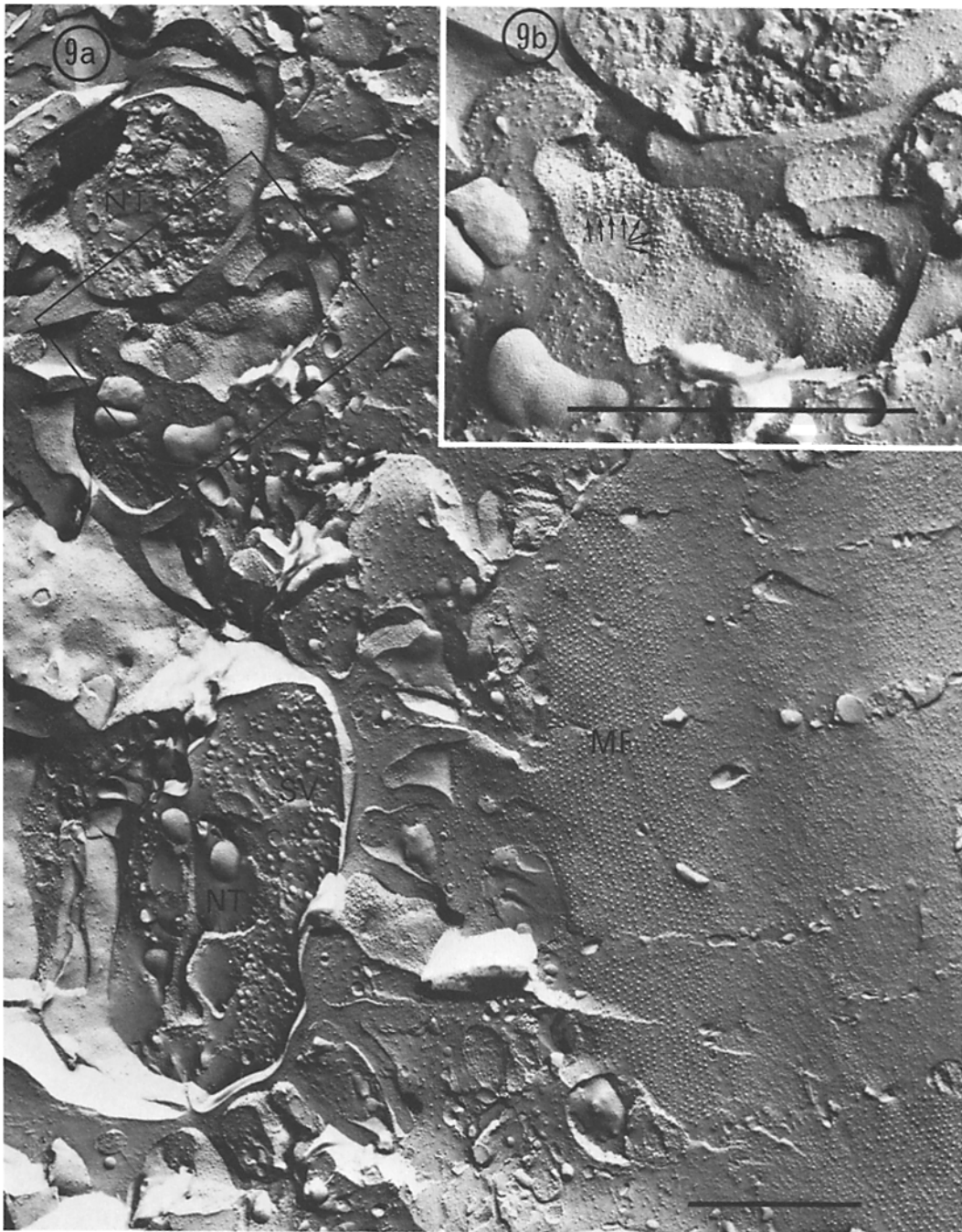
FIGURE 9 (a) Cross fracture of soleus myofiber through endplate region exposing junctional fold membranes. Note vesicles in presynaptic nerve terminals (SV) and myofilaments (MF) in cross fracture. ×
25,000. (b) Higher magnifications of inscribed area in Fig. 7 a. Irregular ("herringbone") rows of particles
are indicated by arrows. × 50,000.

and the cytoplasm in the region of greatest ACh receptor density (arrows) (1, 23). When stained with aqueous uranyl acetate *en bloc*, the subplasmalemmal cytoplasm in the juxtaneural portion of the fold increases in electron density. This electron-dense region can be more adequately assessed with the aid of stereomicrographs prepared in a 1,000 kV electron microscope (Fig. 11 *a*, *b*). Immediately subjacent and "parallel" to the dense portion of the postsynaptic membrane is a filament of approximately 100-Å. Connecting filaments bridge the distance between the "parallel" filament and the dense membrane (approximately 500-Å). These connecting filaments, much like the rungs on a ladder, repeat with an average periodicity of about 250-Å, or approximately the periodicity of the "herringbone rows" of 110–140-Å particles which can be seen in freeze-fracture replicas of the junctional folds. Although these periodic connections emanate from the same "parallel" filament, a stereo visualization of them (Fig. 11 *a*) reveals that they are nonplanar, each attaching to the cortical matrix in a "zig-zag" pattern. It must be emphasized that no direct correlation between these ladder-like filaments and putative ACh receptor complexes observed in freeze-fracture is warranted from these observations. However, we have observed these filaments only in the uppermost regions of junctional fold where ACh receptors have been exclusively localized (23).

Diagrammatic Representations of the Junctional Complexes

Our observations of the macromolecular features common to both fast and slow twitch mammalian neuromuscular junctions are summarized in Fig. 1 and 12. Gross morphological distinctions are observable at low magnification. We have diagrammatically summarized the morphology characteristic of each type of junctional complex in Fig. 1. The consistent features of junctional membranes are represented in Fig. 12. In the illustrated presynaptic membrane (Fig. 12) one sees the paired double rows of 100-Å particles associated with transmitter release. At one such site a vesicle is shown to be attached to the presynaptic membrane between the paired rows of particles. The postsynaptic cholinoceptive membrane is depicted with the characteristic density of irregularly banded 110–140-Å particles. The distribution of these putative receptors is limited to the region of junctional fold nearest the transmitter release sites

of the neurolemma. Beneath the region of receptor-rich postsynaptic membrane is the lattice-work of 100-Å filaments. This filamentous specialization is characteristic of only this portion of junctional fold cytoplasm. In addition, microtubules are usually observed within the junctional folds, occasionally in close proximity to the ladder-like network of filaments.

The junctional morphology is different at a relatively gross level of morphological observation, yet it appears similar at the membrane molecular level. In the nonjunctional sarcolemma the converse is true. Membranes of EDL and soleus which appear similar at low magnification are very different at the membrane molecular level.

Comparisons of the Nonjunctional Sarcolemma of EDL and Soleus

Cleavages of the cylindrical sarcolemma often reveal large expanses of split membrane leaflets (Fig. 13 *a*). At low magnification (Fig. 13 *a*), the protoplasmic fracture faces of both fiber types

FIGURE 10   EDL nerve terminal (*NT*) and top to bottom fracture of muscle junctional fold (*JF*). × 50,000.
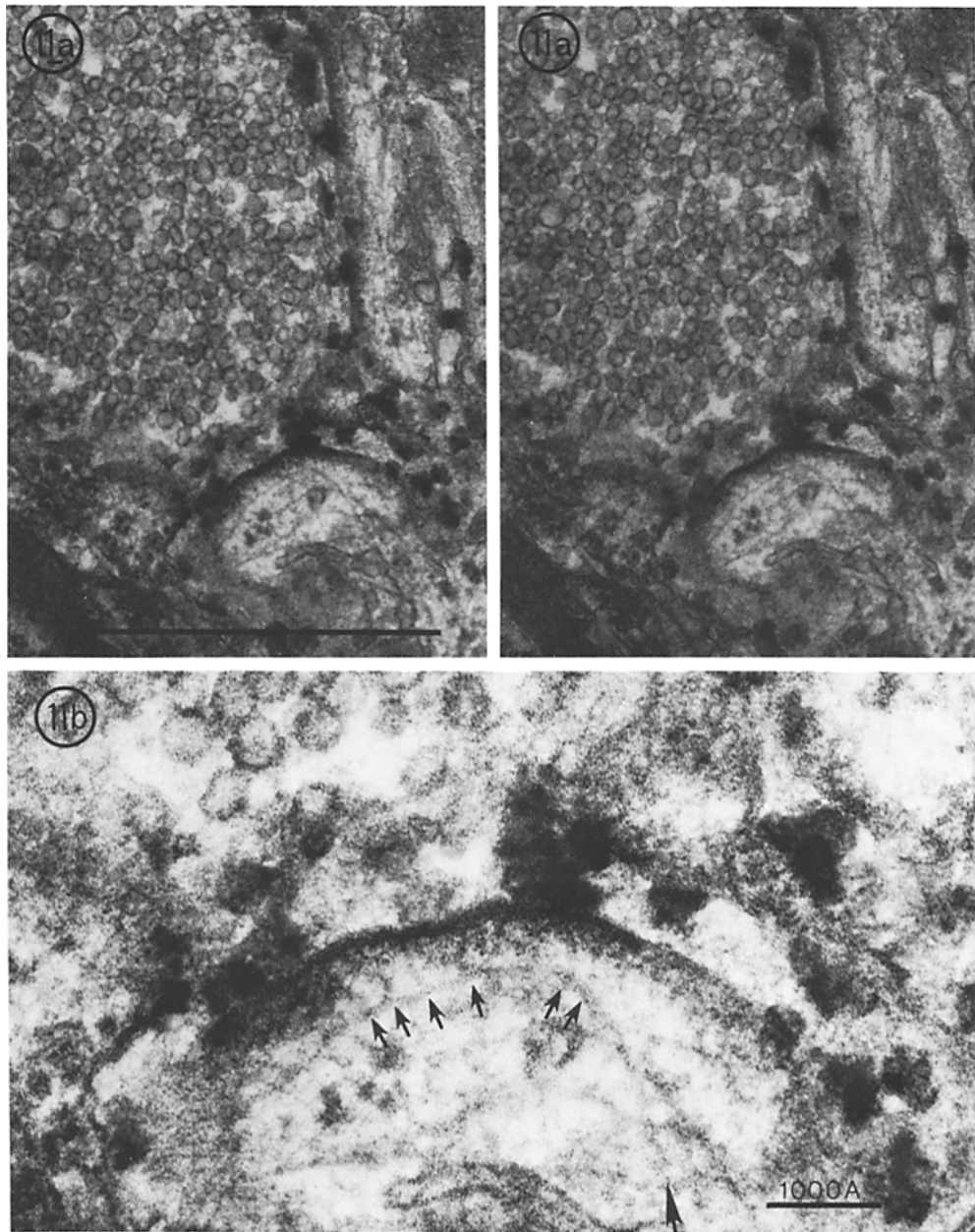
FIGURE 11 (a) Stereo pair of synaptic complex. The reaction product for cholinesterase can be visualized outlining the junctional cleft. The junctional fold at the lower right contains 100-A filaments with periodic projections to the receptor-rich portion of the postsynaptic membrane. The nonplanar projection of these filaments toward the membrane can be appreciated with the aid of stereo visualization. × 50,000; × 100,000 with × 2 stereo viewer. (b) A higher magnification of the specialized membrane region and associated cortical network. × 150,000.

have a regular pattern of repeating elevations and depressions perpendicular to the long axis of the fiber, attributable to the periodicity of the underlying sarcomeres. A portion of the split membrane overlying a sarcomere in Fig. 13a (inscribed area) is presented at higher magnification in Fig. 13b. This particular fracture face is derived from soleus and exhibits a distribution of particles characteris-

tic of fibers from this muscle. There are no organized aggregates of particles apparent in this image (Fig. 13 b) of sarcolemma 0.5–1 mm from the neuromuscular junction, nor are there organized aggregates at 2–4 mm from the soleus junction (Fig. 13 c). This random distribution of particles in soleus is to be contrasted with the square arrays of 60-Å particles in images of EDL membrane leaflets at 0.5–1 mm (Fig. 13 d) and 2–4 mm (Fig. 13 e). These arrays, however, are rarely observed in samples from areas containing stained neuromuscular junctions and, as was shown for diaphragm, are never associated with the folds themselves in mammalian junctions. Whenever a junction is found on a replica an attempt is made to follow and observe the sarcolemma in search of square arrays for as great a distance from the junction as the fiber is identifiable. Cleavages allowing observations of identifiably distant sarcolemma are very rare. The closest we have observed a square array to the edge or a neuromuscular junction, on the same fiber, was 50 μm. Sarco-

lemma within 25 μm of the edge of a junction is more often observed, and has yet to exhibit square arrays in either EDL or soleus. A small portion of an expanse of sarcolemma adjacent to a neuromuscular junction is depicted in Fig. 14.

In previous reports, we presented preliminary descriptions of the fracture faces of rat diaphragm fibers and drew particular attention to these easily recognizable specializations of aggregated 60-Å particles, the "square arrays" (22, 45–47, 49). In the diaphragm, the number and distribution of these specializations was observed to vary as a function of distance from the neuromuscular junction in a nonrandom manner. Our data indicated the possibility of at least two distinct fiber populations in diaphragm, a mixed muscle of both fast and slow contracting fibers. The present study of relatively pure populations of fast and slow twitch fibers found in the rat EDL and soleus muscles clarifies the origin of the bimodal distribution in rat diaphragm.

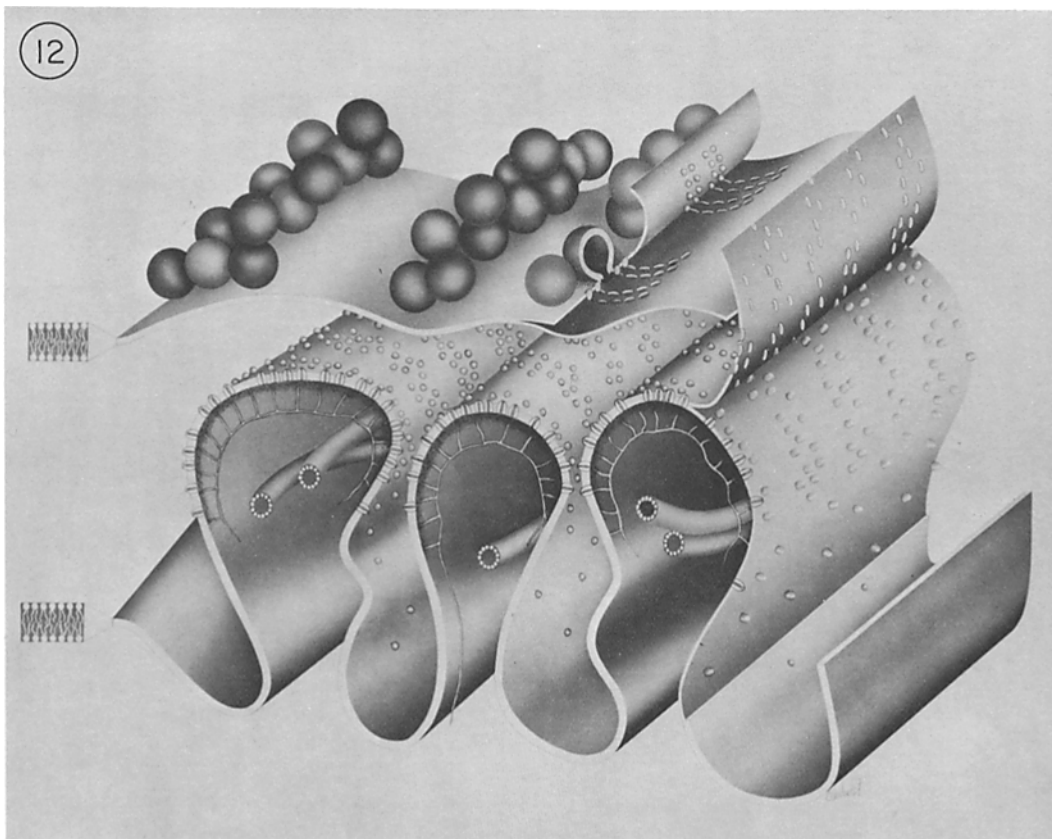For comparison with data obtained from the rat

FIGURE 12   Diagram of consistent features of both EDL and soleus junctions (see text).
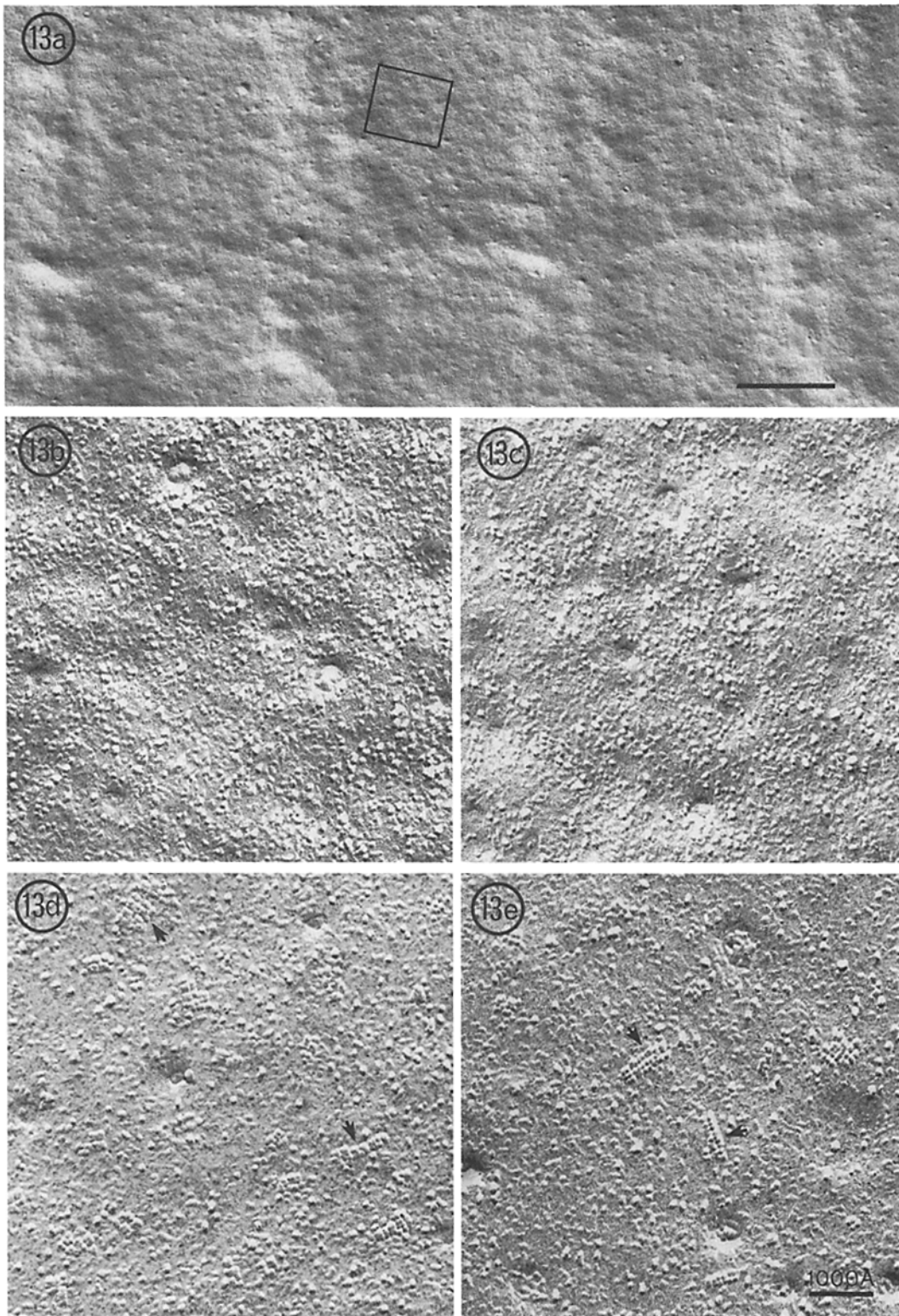
FIGURE 13 (a) A large expanse of cytoplasmic fracture face characteristic of nonjunctional sarcolemmas from soleus. Note the periodic pattern of the three sarcomeres apparent in this figure. × 15,000. (b) At higher magnification of the inscribed area (Fig. 13 a) this protoplasmic fracture face from soleus, 0.5–1 mm from the neuromuscular junction, exhibits a random assortment of particles. × 100,000. (c) An exemplary protoplasmic fracture face from soleus 2–4 mm from the neuromuscular junction. No aggregates of particles are visible. × 100,000. (d) EDL protoplasmic fracture face 0.5–1 mm from the neuromuscular junction with the characteristic high density of square arrays. × 100,000. (e) A similar EDL sarcolemma, 2–4 mm from the neuromuscular junction. Fewer arrays per micrometer are apparent. × 100,000.

diaphragm, we examined cleaved membrane surfaces of EDL and soleus within 100 μm, at 0.5-1 mm, and 2-4 mm from the neuromuscular junction. The data were tabulated and the number of characteristic square arrays per square micrometer determined (Fig. 15). At least 150 μm² were counted for each of the areas represented.

FIGURE 14 A fracture of the sarcolemma immediately adjacent to a neuromuscular junction in EDL. This protoplasmic fracture face demonstrates the junctional specificity of the rows of putative receptor particles (several marked with arrows). Square arrays appear to be absent from the junctional region visible here, and at greater distances from the neuromuscular junction (to approximately 50 μm). × 50,000.

The occurrence of square arrays appears to be a function of which muscle is observed and, in EDL where arrays regularly occur, their density is a function of the distance from the neuromuscular junction. At distances greater than 50 μm from the edge of a neuromuscular junction, the number of arrays appears to increase in EDL fibers up to a density of 15-30/μm² at distances of 0.5-1 mm (500-1000 μm) (Fig. 15; also see Fig. 13 d). Replicas of samples from EDL fibers at greater distances (2-4 mm from the neuromuscular junction) demonstrate a decrease in square array density (approximately 3-15/μm²) (Fig. 15; also see Fig. 13 e). Extensive examination of sarcolemma near the neuromuscular junction of soleus fibers and at distances of 0.5-1 mm and 2-4 mm has revealed a virtual absence of square arrays (see graph, Fig. 15; also Fig. 13 b, c). Square arrays were actually observed on fewer than 10% of the soleus samples, and, even when present, were usually at a lower density than on EDL. The observed densities were either 0/μm² (more than 40 fibers), less than 5/μm² (three fibers), or between 10 and 25/μm² (two fibers). These sarcolemmal specializations which differ dramatically between EDL and soleus fibers thus comprise a new parameter which may be of general significance in defining the differences in functional membrane properties of fast and slow twitch muscle, at least as represented by the tonically and phasically innervated rat soleus and EDL (18).

Landis and Reese (31) and Dermietzel (14) have noted the occurrence of similar arrays of particles in membranes of brain astrocytes. In particular, the membranes of astrocytic end feet adjacent to and surrounding the brain capillaries were more densely populated with square arrays than other areas of the astrocyte membrane. No perivascular aggregations of square arrays were observed in this study of muscle fibers. The aggregation of this structure near capillary endothelium may then be an interesting peculiarity of certain cells in neural tissue, perhaps reflecting the high ATPase activity of these membranes (58).

DISCUSSION

Morphological Differences and Similarities in the Neuromuscular Junction of Mammalian Fast and Slow Twitch Muscle

Ultrastructural variations between fiber types have been described for the myoneural junctions in

EXTENSOR DIGITORUM LONGUS
(fast twitch)

square arrays / μm^2

30
25
20
15
10
5
0

NMJ containing samp.   1/2-1mm samples   2-4mm samples

(each • represents 5μm^2 of micrographs from A face replicas counted for square arrays)

SOLEUS
(slow twitch)

square arrays / μm^2

30
25
20
15
10
5
0

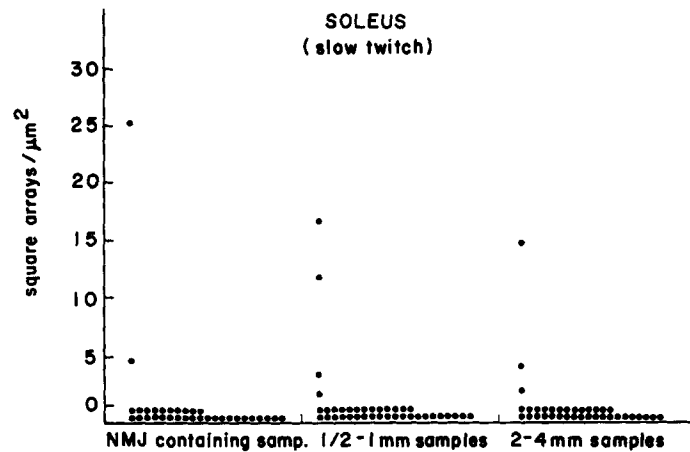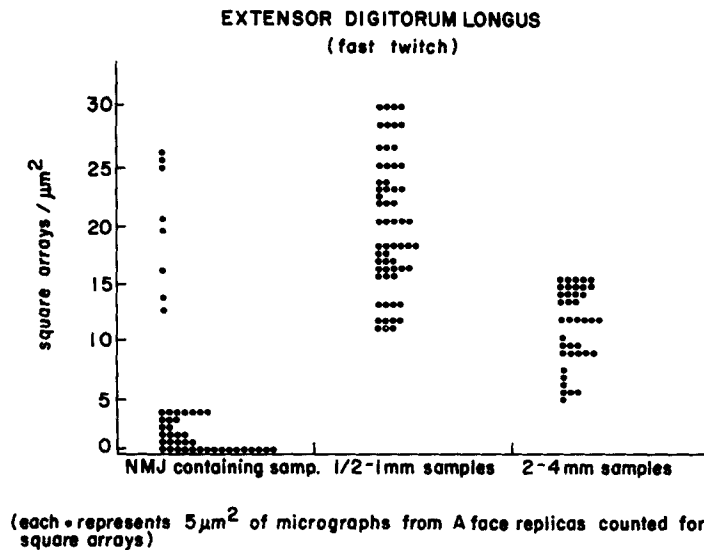NMJ containing samp.   1/2-1 mm samples   2-4mm samples

FIGURE 15   Graphic representation of observed square array density in both EDL and soleus as a function of distance from the neuromuscular junction. (For details, see text.)

diaphragm and intercostal muscles of the rat (40, 41). The size of the neuromuscular junction has been shown to be proportional to the diameter of the muscle fiber (39) and to the frequency of spontaneous miniature endplate potentials (35). We have confirmed the existence of endplate morphologies which are characteristically distinguishable in fibers differing in contractile properties. These gross structural differences are not apparent, however, at the membrane molecular level. For example, the *presynaptic* membranes in both fast and slow twitch neuromuscular junctions exhibit similar paired double rows of particles opposite the openings of the secondary synaptic clefts. Disruptions of the membrane associated with nerve stimulation occur predominantly between these paired rows of particles. With two notable differences, these specialized regions of mammalian junctions resemble the "active zones" recently described in frog motor endplates (13, 28, 42). First, the comparatively short "railroad track" rows of particles in mammalian endplates are oriented perpendicular to the long axis of the junctional folding, whereas the long rows of frog active zones are parallel to the fold axis. Second, in mammalian junctions tranmitter release-related

perturbances are observed between the pairs of railroad tracks, whereas in amphibia analogous events occur lateral to the four-row assemblage.

We emphasize that, despite the differing patterns of neuronal firing in EDL and soleus, the apparent transmitter release sites are identical both in the size and in the spacing of particles. Moreover, differences in the pattern of nerve firing and the resultant endplate depolarization apparently do not result in differences in acetylcholine sensitivity of the junctional membrane (1). This lack of difference is not a trivial point.

The alpha motor neuron innervating the fast twitch fiber fires infrequently, but in rapid bursts of 30–60 impulses/s. During this "phasic" activity there is rapid release of ACh, resulting in brief flooding of the receptor sites, initiating their activation, followed by activation of the contractile process 30-60 times/s. In contrast, the alpha motor neurons innervating slow twitch fibers fire rhythmically and continuously for relatively long periods of time. These "tonic" discharges of neurons innervating the slow twitch fibers occur at a lower frequency (10–20 impulses/s) than those involved in the bursts of impulses from motor neurons supplying the fast twitch fibers (18). Even though these different junctions are washed with different quantities of ACh at different intervals, their sensitivities to applied ACh and the density of receptors in the postsynaptic membrane are the same (1). It appears that the quantitative difference between phasic and tonic stimulation is insufficient to induce alterations in the density of receptors or the iontophoretic ACh sensitivity of postsynaptic membrane. In both types of fibers, particles of the junctional folds presumed to represent ACh receptor complexes are identical in size, distribution, and packing density, and are arranged in similar corrugated, herringbone rows. (Differences in sarcolemmal composition will be considered in a later section.)

Possible Mechanisms Regulating the Apparently Maximal Aggregation of Receptors

Nerve muscle interaction would be most efficiently facilitated if the synaptic vesicle release sites were in very close proximity to receptors, if the receptors were at an optimal density at the release sites, and if receptors were not inserted in unnecessary locations. One would assume that both types of cells independently or cooperatively would utilize mechanisms to effect this organization.

The search for mechanisms responsible for the control of receptor spread is a central topic in contemporary neurobiology. The flow of fluorescein-labeled sarcolemmal antigens has been observed in rat muscle culture, and a "diffusion constant" of 10^{-9} cm/s calculated for these embryonic cells (19). One might hypothesize that a mechanism has been evolved to promote receptor organization at the top of the folds and to restrict diffusion of the receptors away from these regions. The subplasmalemmal array of filaments and ladder-like projections observed to be associated with or attached to the membrane regions of highest receptor density may serve this function. It should be noted that other fiber-membrane particle associations have been reported in the luminal plasma membrane of the urinary bladder (55) and in erythrocyte membrane (21). These studies provide evidence for the hypothesis that the distribution of membrane particles can be controlled by cortical filament networks. No direct connection of receptor complex and 100-Å filament is demonstrated in this report. However, the "herringbone" arrangement of putative receptor complexes and the periodic nature of the filament network do suggest some direct or indirect interaction.

The Reliability of Neuromuscular Transmission

The morphological consistencies in pre- and postsynaptic particulate specializations can be considered in relation to quantitative aspects of neuromuscular transmission. Using autoradiographic techniques, for example, Salpeter et al. (51) have determined that the density of acetylcholinesterase per square micrometer of fold and the concentration of acetylcholinesterase per cubic micrometer of cleft volume are identical for various types of muscle. Salpeter and Eldefrawi (50) reported that the quantity of AChE present for the hydrolysis of ACh is approximately one-half to one-third the concentration of receptor near the plane of the membrane, and that this relationship is apparently consistent for endplates of muscles with various contractile properties (50). Their calculations showing the concentration of ACh released in the cleft to be in excess of that needed for maximal response of the receptor, coupled with additional kinetic considerations, allowed them to

conclude that the design of the endplate includes an adequate "safety factor" such that, under normal physiological conditions, a nerve action potential invariably results in a muscle endplate potential. The estimates of this safety factor were made assuming an equal distribution of receptor over the total folded membrane area. Reconsideration of the diffusion effects on local cleft concentrations of ACh is appropriate, however, due to demonstration of an ordered aggregation of receptors (bungarotoxin binding sites, freeze-fractured particles) at the tops of junctional folds (22, 23, 42, 45, 46). Such an increase in concentration would aid the kinetic arguments of Salpeter and Eldefrawi (50), resulting in an increase in the magnitude of this safety factor. Increased efficiency of the transmission mechanism may also be gained by preferential release of ACh at locations consistently related to the junctional folding. The presynaptic rows of particles of the mammalian nerve terminal observed in opposition to the junctional clefts (22) and those observed in amphibia (16, 28, 42) suggest the development of such preferential sites of release in both mammalian fast and slow twitch myoneural junctions as well as amphibian motor endplates.

Relationship Between Square Arrays and Fiber Types

In the late 19th century, Ranvier (43, 44) observed striking differences in the appearance and contractile properties of various vertebrate skeletal muscles. He noted that the medial gastrocnemius muscle (a white fast twitch muscle) appeared lighter and exhibited a faster contraction rate, a higher fusion rate, and earlier fatigue than the soleus (a red slow twitch muscle). Subsequently, many investigators have attempted to refine this early description of the contractile and biochemical properties of muscle. Unfortunately, not only was this correlation of contraction rate, fiber color, and degree of fatigability proven to be an oversimplification, but it has also never been demonstrated that contraction rate can be uniquely correlated with any basic property other than myosin ATPase activity. For example, many muscles homogeneous in contraction rates have been demonstrated to exhibit heterogeneity in oxidative enzyme staining, mitochondrial content, mitochondrial orientation, and extent of vascularization (20, 24–26, 50).

Since we observed what appeared to be at least two distinct classes of fibers on the basis of number

and distribution of square arrays in the rat diaphragm, and since the rat diaphragm is a "mixed muscle" containing a variety of fiber types (according to various classification schemes), we thought it reasonable to examine muscles with relatively pure populations (by any one method of classification) to determine if the arrays were constantly and uniquely associated with any single fiber type. To this end, we have examined rat and mouse intercostal, medial and lateral gastrocnemius, soleus, extensor digitorum longus, flexor digitorum brevis, and human medial gastrocnemius, intercostal and biceps. Although square arrays were observed on at least some fibers for each of these muscles, we observed the highest positive and negative correlations on fibers from the uniformly fast EDL and predominantly slow soleus.

The presence of square arrays appears to vary directly with the observed differences in isometric twitch contraction times reported by Close (11) for rat EDL and soleus. He describes three classes of motor units defined by contraction time. The fastest contractions are elicited by all units stimulated in EDL. Soleus, on the other hand, exhibited slow contractions in 90% of the units stimulated, the remaining 10% being intermediate in contraction time. The close correlation of these results with the distribution of square arrays on rat EDL and soleus indicate that the presence or absence of this membrane specialization may be directly correlated with whether the muscle is fast or slow in contraction time, or, alternatively, with phasic or tonic activation. Thus, despite heterogeneity of both EDL and soleus with respect to metabolic properties (25), the square arrays appear to be present in large numbers on fast twitch fibers (whether "intermediate" or "white") and virtually nonexistent on slow twitch fibers (whether "red" or "intermediate").

Metabolic Properties vs. Contractile Properties

Metabolic differentiation appears to be a mechanism by which fibers increase their endurance to periods of prolonged exercise and is accomplished by increasing the muscle's capacity to rely on oxidative metabolism (5, 33). However, prolonged exercise does not result in alterations of contractile properties (6). Fibers classified on the basis of metabolic histochemistry, mitochondrial content, and extent of vascularization appear to reside on a

continuum between the extremes of development for either glycolytic or oxidative metabolism. Quantification and comparison of square array distribution between rat EDL and soleus presented in this report *does not* generate such a continuum, and thus the bimodal distribution observed is unrelated to any continuous classification scheme.

Metabolic histochemistry on rat soleus reveals at least two classes of fibers (56). Of these, 20% are categorized as "red" and 80% as "intermediate" by a classification scheme which combines histochemistry with mitochondrial quantification (25). This same analysis, when applied to rat EDL, results in observations of three cytologically distinguishable fiber types (cf. 25). Significantly, we did not observe the presence of square arrays in a trimodal distribution of fibers in EDL or soleus. On the contrary, EDL fibers uniformly exhibited high numbers of square arrays in nonjunctional sarcolemma (greater than 100 μm from the neuromuscular junction), whereas approximately 90% of soleus sarcolemma examined had none. The clear difference in the number and distribution of square arrays in fibers from these two muscles does not correlate with the proportions of "red," "intermediate," and "white" fibers. Therefore, we conclude that their presence is not correlated with metabolic fiber classification systems but is uniquely and directly associated with another property such as twitch and/or contraction time, or perhaps, the pattern of motor innervation and the resultant sarcolemmal depolarization patterns. We emphasize that we are not attempting to redefine previous classification schemes. On the contrary, apparently we have observed a class of membrane integral proteins (the square arrays) whose distribution appears to reflect differences in basic membrane properties of fast and slow twitch muscle fibers.

Regulation of the differing speeds of contraction observed in fast and slow twitch muscle is apparently accomplished by variations in the rate of hydrolysis of ATP by myosin (3, 4, 27). The speed of contraction and presence of kinetically distinct myosin ATPase has been correlated directly with the characteristics of the innervating neuronal activity (3, 9, 10). Differences in electrogenic Na^+/K^+ pumping have also been demonstrated between soleus and EDL (15, 32). Our morphological observations of sarcolemmal differentiation between fiber types implicate a correlated physiological differentiation. The dependence of this as yet unidentified membrane property upon the characteristics of the innervating neuronal activity may also be an interesting consideration.

Are Square Arrays Involved in Excitability?

Square arrays apparently similar to those described in skeletal muscle (22, 45–47, 49, 52) and cardiac muscle (36) are observed on cells that do not conduct propagated action potentials. They have been found in the lateral plasma membranes of intestinal epithelial cells (54), on brain astrocytes (14, 31), in hepatocyte plasma membranes (30), and in the basal and lateral surfaces of the light cells of kidney collecting tubule (29). Staehelin's (54) early speculations that the square arrays might present a special third type of gap junction have subsequently been rendered inoperable because the arrays appear on cell surfaces separated by large spaces and thick intervening basement membranes (49).

Since the square arrays have been observed in cells that do not conduct propagated action potentials, it seems unlikely that they play an active role in conductance of depolarization in muscle. Perhaps in this regard it would be instructive to re-examine the observations of Torack and Barrnett (58) and Marchesi et al. (34) concerning the electron microscope localization of "ATPase" in rat brain. In these studies high levels of ATPase reaction products were observed along the perivascular surfaces of the astrocytic end feet, perhaps not coincidentally where the "square arrays" have been observed in greatest abundance (31). Nevertheless, the present data indicate that sarcolemmas of EDL and soleus fibers may provide an appropriate material for differential biochemical analysis and subsequent isolation and characterization of these interesting membrane components.

CONCLUSION

Thin sections confirm the existence of morphological differences between synaptic complexes of fast and slow twitch fibers, but in freeze-fracture preparations no fiber-specific distinctions can be made between the EDL and soleus junctional specializations associated with transmitter release or ACh receptivity. It is hypothesized that the observed arrangement of putative receptor complexes in characteristic irregular rows may be dictated by a network of 100-Å filaments and ladder-like bridges observed in high voltage stereo

micrographs of the juxtaneural portions of the folds. We demonstrate that the differentiations of fast and slow twitch fibers are not reflected in the micromorphology of their synaptic membranes, but that differences can be observed in the macromolecular organization of their nonjunctional electrically excitable sarcolemmas. Thus, differences in the macromolecular architecture of the membranes of fast and slow twitch fibers occur in the electrically excitable nonjunctional sarcolemma but apparently not in the synaptic

REFERENCES

1. Albuquerque, E. X., E. A. Barnard, C. W. Porter, and J. E. Warnick. 1974. The density of acetylcholine receptors and their sensitivity in the postsynaptic membrane of muscle endplates. *Proc. Natl. Acad. Sci. U. S. A.* **71**:2818-2822.

2. Albuquerque, E. X., and R. J. McIsaac. 1970. Fast and slow mammalian muscles after denervation. *Exp. Neurol.* **26**:183-202.

3. Barany, M. 1967. ATPase activity of myosin correlated with speed of muscle shortening. *J. Gen. Physiol.* **50**:197-218.

4. Barany, M., K. Barany, T. Reckard, and A. Volpe. 1965. Myosin of fast and slow muscles of the rabbit. *Arch. Biochem. Biophys.* **109**:185-191.

5. Barnard, R. J., V. R. Edgerton, and J. B. Peter. 1970. Effect of exercise on skeletal muscle. I. Biochemical and histochemical properties. *J. Appl. Physiol.* **28**:762-766.

6. Barnard, R. J., V. R. Edgerton, and J. B. Peter. 1970. Effect of exercise on skeletal muscle. II. Contractile properties. *J. Appl. Physiol.* **28**:767-770.

7. Branton, D., S. Bullivant, N. B. Gilula, M. J. Karnovsky, H. Moor, K. Mühlethaler, D. H. Northcote, L. Packer, B. Satir, P. Satir, V. Speth, L. A. Staehelin, R. L. Steere, and R. S. Weinstein. 1975. Freeze-etching nomenclature. *Science (Wash. D.C.)*. In press.

8. Brooke, M. H., and K. K. Kaiser. 1974. The use and abuse of muscle histochemistry. *Ann. N. Y. Acad. Sci.* **228**:121-144.

9. Buller, A. J., J. C. Eccles, and R. M. Eccles. 1960. Differentiation of fast and slow muscles in the cat hind limb. *J. Physiol. (Lond.).* **150**:399-416.

10. Buller, A. J., J. C. Eccles, and R. M. Eccles. 1960. Interactions between motorneurons and muscles in respect of the characteristic speeds of their response. *J. Physiol. (Lond.).* **150**:417-439.

11. Close, R. 1967. Properties of motor units in fast and slow muscles of the rat. *J. Physiol. (Lond.).* **193**:45-55.

12. Close, R. L. 1972. Dynamic properties of mammalian skeletal muscles. *Physiol. Rev.* **52**:129-197.

13. Couteaux, R., et M. Pécot-Dechauvassine. 1970. Vesicules synaptiques et poches au niveau des "zones actives" de la jonction neuromusculaire. *C. R. Hebd. Séances Acad. Sci. (Paris).* **271D**:2346-2349.

14. Dermietzel, R. 1973. Visualization by freeze-fracturing of regular structures in glial cell membranes. *Naturwissenschaften.* **60**:208.

15. Dockry, M., R. P. Kernan, and A. Tangney. 1966. Active transport of sodium and potassium in mammalian skeletal muscle and its modification by nerve and by cholinergic and adrenergic agents. *J. Physiol. (Lond.).* **186**:187-200.

16. Dreyer, F., K. Peper, K. Akert, C. Sandri, and H. Moor. 1973. Ultrastructure of the "active zone" in the frog neuromuscular junction. *Brain Res.* **62**:373-380.

17. Dubowits, V., and A. G. E. Pearse. 1960. A comparative histochemical study of oxidative enzyme and phosphorylase activity in skeletal muscle. *Histochemie.* **2**:105-117.

18. Eccles, J. C., R. M. Eccles, and A. Lundberg. 1958. The action potentials of the alpha motoneurons supplying fast and slow muscles. *J. Physiol. (Lond.).* **142**:275-291.

19. Edidin, M., and D. Fambrough. 1973. Fluidity of the surface of cultured muscle fibers—rapid lateral diffusion of marked surface antigens. *J. Cell Biol.* **57**:27-37.

20. Eisenberg, B. R., A. M. Kuda, and J. B. Peter. 1974. Stereological analysis of mammalian skeletal muscle. I. Soleus muscle of the adult guinea pig. *J. Cell Biol.* **60**:732-754.

21. Elgsaeter, A., and D. Branton. 1974. Intramembrane particle aggregation in erythrocyte ghosts. I. The effects of protein removal. *J. Cell Biol.* **63**:1018-1030.

22. Ellisman, M. E., J. E. Rash, L. A. Staehelin, and K. R. Porter. 1974. Freeze-fracture comparisons of the neuromuscular junction and postjunctional sarcolemmas of mammalian fast and slow twitch muscle fibers. *J. Cell Biol.* **63** (2, Pt. 2):93 a. (Abstr.).

23. Fertuck, H. C., and M. M. Salpeter. 1974. Localization of acetylcholine receptor by 125I-labeled bungarotoxin binding at mouse motor endplates. *Proc. Natl. Acad. Sci. U. S. A.* **71**:1376-1378.

24. Gauthier, G. F. 1970. The ultrastructure of three fiber types in mammalian skeletal muscle. *In* The Physiology and Biochemistry of Muscle as a Food. E. J. Briskey, R. G. Cassens, and B. B. Marsh,

editor., Vol. 2. University of Wisconsin Press, Madison, Wis. 103.

25. GAUTHIER, G. F. 1971. The structural and cytochemical heterogeneity of the mammalian skeletal muscle fibers. *In* Contractility of Muscle Cells and Related Processes. R. J. Podolsky, editor. Prentice-Hall Inc., Eaglewood Cliffs, N.J. 131.

26. GAUTHIER, G. F., and H. A. PADYKULA. 1966. Cytological studies of fiber types in skeletal muscles. A comparative study of the mammalian diaphragm. *J. Cell Biol.* **28**:333-354.

27. GUTH, L., and F. J. SAMAHA. 1969. Qualitative differences between actomyosin ATPase of slow and fast mammalian muscle. *Exp. Neurol.* **25**:138-152.

28. HEUSER, J. E., T. S. REESE, and M. D. LANDIS, 1974. Functional changes in frog neuromuscular junctions studied with freeze-fracture. *J. Neurocytol.* **3**:108-131.

29. HUBERT, F., C. PRICAM, A. PERRELET, and L. ORCI. 1975. Specific plasma membrane differentiations in the cells of the collecting tubule. *J. Ultrastruct. Res.* **52**:13-20.

30. KREUTZIGER, G. O. 1968. Freeze-etching of intercellular junctions of mouse liver. *In* Proceedings of the 26th Meeting of the Electron Microscope Society of America. Claitor's Publishing Div., Baton Rouge, La. 234.

31. LANDIS, D. M. D., and T. S. REESE. 1974. Arrays of particles in freeze-fractured astrocytic membranes. *J. Cell Biol.* **60**:316-320.

32. LOCKE, S., and H. C. SOLOMON. 1967. Relation of resting potential of rat gastrocnemius and soleus muscles to innervation, activity and the Na-K pump. *J. Exp. Zool.* **166**:377-386.

33. MAI, J., V. R. EDGERTON, and R. J. BARNARD. 1970. Capillary of red, white and intermediate fibers after training. *Experientia (Basel).* **26**:1222-1223.

34. MARCHESI, V. T., M. V. SEARS, and R. J. BARRNETT. 1964. Electron microscopic studies of nucleoside phosphatase activity in blood vessels and glia of the retina. *Invest. Opthal. Mol.* **3**:1-21.

35. MCARDLE, J. J., and E. X. ALBUQUERQUE. 1973. A study of the reinnervation of fast and slow mammalian muscles. *J. Gen. Physiol.* **61**:1-23.

36. MCNUTT, S. N. 1975. Ultrastructure of the myocardial sarcolemma. *Circ. Res.* **37**:1-13.

37. MILEDI, R., and J. ZELENA. 1966. Sensitivity to acetylcholine in rat slow muscle. *Nature* (Lond.). **210**:855-856.

38. NACHMIAS, V. T., and H. A. PADYKULA. 1958. A histochemical study of normal and denervated red and white muscles of the rat. *J. Biophys. Biochem. Cytol.* **4**:47-57.

39. NYSTROM, B. 1968. Histochemistry of developing cat muscle. *Acta Neurol. Scand.* **44**:405-439.

40. OGATA, T., T. HONDO, and T. SEITO. 1967. An electron microscopic study on differences in the fine structure of motor endplate in red, white and

intermediate muscle fibers of rat intercostal muscle. A preliminary study. *Acta Med. Okayama.* **21**:327.

41. PADYKULA, H. A., and G. F. GAUTHIER. 1970. The ultrastructure of the neuromuscular junctions of mammalian red, white and intermediate skeletal muscle fibers. *J. Cell Biol.* **46**:27-41.

42. PEPER, K., F. DREYER, C. SANDRI, K. AKERT, and H. MOOR. 1974. Structure and ultrastructure of the frog motor endplate: a freeze-etching study. *Cell Tissue Res.* **149**:437-455.

43. RANVIER, L. 1874. De quelque faits relatifs á l'histologie et á la physiologie des muscles striés. *Arch. Physiol. Norm. Pathol.* **2** Ser. I: 5-15.

44. RANVIER, L. 1880. Leconus d'Anatomie Generale sur le Systeme Musculaire. Delahaye, Paris.

45. RASH, J. E., and M. H. ELLISMAN. 1974. Studies of excitable membranes. I. Macromolecular specializations of the neuromuscular junction and the nonjunctional sarcolemma. *J. Cell Biol.* **63**:567-586.

46. RASH, J. E., M. H. ELLISMAN, and L. A. STAEHELIN. 1973. Freeze-cleaved neuromuscular junctions: macromolecular architecture of postsynaptic membranes of normal vs. denervated muscle. *J. Cell Biol.* **59** (2, Pt. 2):280 a. (Abstr.).

47. RASH, J. E., M. H. ELLISMAN, L. A. STAEHELIN, and K. R. PORTER. 1974. Specializations of excitable membranes in normal, chronically denervated, and dystrophic muscle fibers. *In* Exploratory Concepts in Muscle (II) Control Mechanisms in Development and Function of Muscle and Their Relationship to Muscular Dystrophy and Related Neuromuscular Diseases. Muscular Dystrophy Association of America, New York. Excerpta Medica, Amsterdam 271-289.

48. RASH, J. E., J. W. SHAY, and J. J. BIESELE. 1968. Urea extraction of Z bands, intercalated disks, and Desmosomes. *J. Ultrastruct. Res.* **24**:181-189.

49. RASH, J. E., L. A. STAEHELIN, and M. H. ELLISMAN. 1974. Rectangular arrays of particles on freeze-cleaved plasma membranes are not gap junctions. *Exp. Cell Res.* **86**:187-190.

50. SALPETER, M. M., and M. E. ELDEFRAWI. 1973. Sizes of endplate compartments, densities of acetylcholine receptor and other quantitative aspects of neuromuscular transmission. *J. Histochem. Cytochem.* **21**:769-778.

51. SALPETER, M. M., H. PLATTNER, and A. W. ROGERS. 1972. Quantitative assay of esterases in endplates of mouse diaphragm by electron microscope autoradiography. *J. Histochem. Cytochem.* **20**:1059-1068.

52. SMITH, D. S., R. J. BAERWALD, and M. A. HART. 1975. The distribution of orthogonal assemblies and other intercalated particles in frog sartorius and rabbit sarcospinalis muscle. *Tissue Cell.* **7**:69-382.

53. SRETER, F. A., J. GERGELY, S. SALMONS, and F. ROMANUL. 1973. Synthesis by fast muscle of myosin light chains characteristic of slow muscle in response

to long-term stimulation. *Nat. New Biol.* **241**:17-19.

54. STAEHELIN, L. A. 1972. Three types of gap junctions interconnecting intestinal epithelial cells visualized freeze-etching. *Proc. Natl. Acad. Sci. U. S. A.* **69**: 1318-1321.

55. STAEHELIN, L. A., F. J. CHLAPOWSKI, and M. A. BONNEVILLE. 1972. Lumenal plasma membrane of the urinary bladder. I. Three-dimensional reconstruction from freeze-etch images. *J. Cell Biol.* **53**:73-91.

56. STEIN, J. M., and H. A. PADYKULA. 1962. Histochemical classification of individual skeletal muscle fibers of the rat. *Am. J. Anat.* **110**:103-115.

57. STEMPAK, J. G., and R. T. WARD. 1964. An improved staining method for electron microscopy. *J. Cell Biol.* **22**:697-701.

58. TORACK, R. M., and R. J. BARRNETT. 1964. The fine structural localization of nucleoside phosphate activity in the blood-brain barrier. *J. Neuropathol. Neurol.* **23**:46.

59. VENABLE, J. H., and R. A. COGGESHALL. 1965. A simplified lead citrate stain for use in electron microscopy. *J. Cell Biol.* **25**:407-408.